

This is an Open Access document downloaded from ORCA, Cardiff University's institutional repository: <https://orca.cardiff.ac.uk/id/eprint/101758/>

This is the author's version of a work that was submitted to / accepted for publication.

Citation for final published version:

Taban, Ismail M., Zhu, Jinge, DeLuca, Hector F. and Simons, Claire 2017. Synthesis, molecular modelling and CYP24A1 inhibitory activity of novel of (E)-N-(2-(1H-imidazol-1-yl)-2-(phenylethyl)-3/4-styrylbenzamides. *Bioorganic and Medicinal Chemistry* 25 (15) , pp. 4076-4087.
10.1016/j.bmc.2017.05.055

Publishers page: <http://dx.doi.org/10.1016/j.bmc.2017.05.055>

Please note:

Changes made as a result of publishing processes such as copy-editing, formatting and page numbers may not be reflected in this version. For the definitive version of this publication, please refer to the published source. You are advised to consult the publisher's version if you wish to cite this paper.

This version is being made available in accordance with publisher policies. See <http://orca.cf.ac.uk/policies.html> for usage policies. Copyright and moral rights for publications made available in ORCA are retained by the copyright holders.



**Synthesis, molecular modelling and CYP24A1 inhibitory activity of novel
of (*E*)-*N*-(2-(1*H*-imidazol-1-yl)-2-(phenylethyl)-3/4-styrylbenzamides**

Ismail M. Taban,^a Jinge Zhu,^b Hector F. DeLuca^b and Claire Simons^{a*}

^aMedicinal Chemistry, School of Pharmacy & Pharmaceutical Sciences, Cardiff University,
King Edward VII Avenue, Cardiff CF10 3NB, UK; ^bDepartment of Biochemistry, University
of Wisconsin-Madison, 433 Babcock Drive, Madison, WI 53706-1544, USA.

Corresponding author: Tel.: +44 (0) 2920 876307; fax: +44 (0) 2920 874149.

E-mail address: simonsc@cardiff.ac.uk (C. Simons)

Key words:

Vitamin D

(E)-*N*-(2-(1*H*-imidazol-1-yl)-2-(phenylethyl)-3/4-styrylbenzamides

CYP24A1

Enzyme inhibition

Molecular modelling

Abstract

CYP24A1 (25-hydroxyvitamin D-24-hydroxylase) is a useful enzyme target for a range of medical conditions including cancer, cardiovascular and autoimmune disease, which show elevated CYP24A1 levels and corresponding reduction of calcitriol (the biologically active form of vitamin D). A series of *(E)*-*N*-(2-(1*H*-imidazol-1-yl)-2-(phenylethyl)-3/4-styrylbenzamides have been synthesised using an efficient synthetic route and shown to be potent inhibitors of CYP24A1 (IC₅₀ 0.11-0.35 μ M) compared with the standard ketoconazole. Molecular modelling using our CYP24A1 homology model showed the inhibitors to fill the hydrophobic binding site, forming key transition metal interaction between the imidazole nitrogen and the haem Fe³⁺ and multiple interactions with the active site amino acid residues.

1. Introduction

Vitamin D is the starting compound of an endocrine system, and plays a principal role in the maintenance of calcium and phosphate homeostasis and is essential for the maintenance of a healthy skeleton¹. Vitamin D is produced in the epidermis from 7-dehydrocholesterol, by sunlight or UV light. Vitamin D can also be obtained from dietary sources. Previtamin D₃ is produced by the opening of the steroid nucleus (B ring broken by UV light with spectrum 280 - 320 nm²). Previtamin D₃ isomerises into Vitamin D₃³. Additionally the three most important steps in vitamin D metabolism, 25-hydroxylation, 1 α -hydroxylation, and 24-hydroxylation are all performed by cytochrome P450 enzymes⁴.

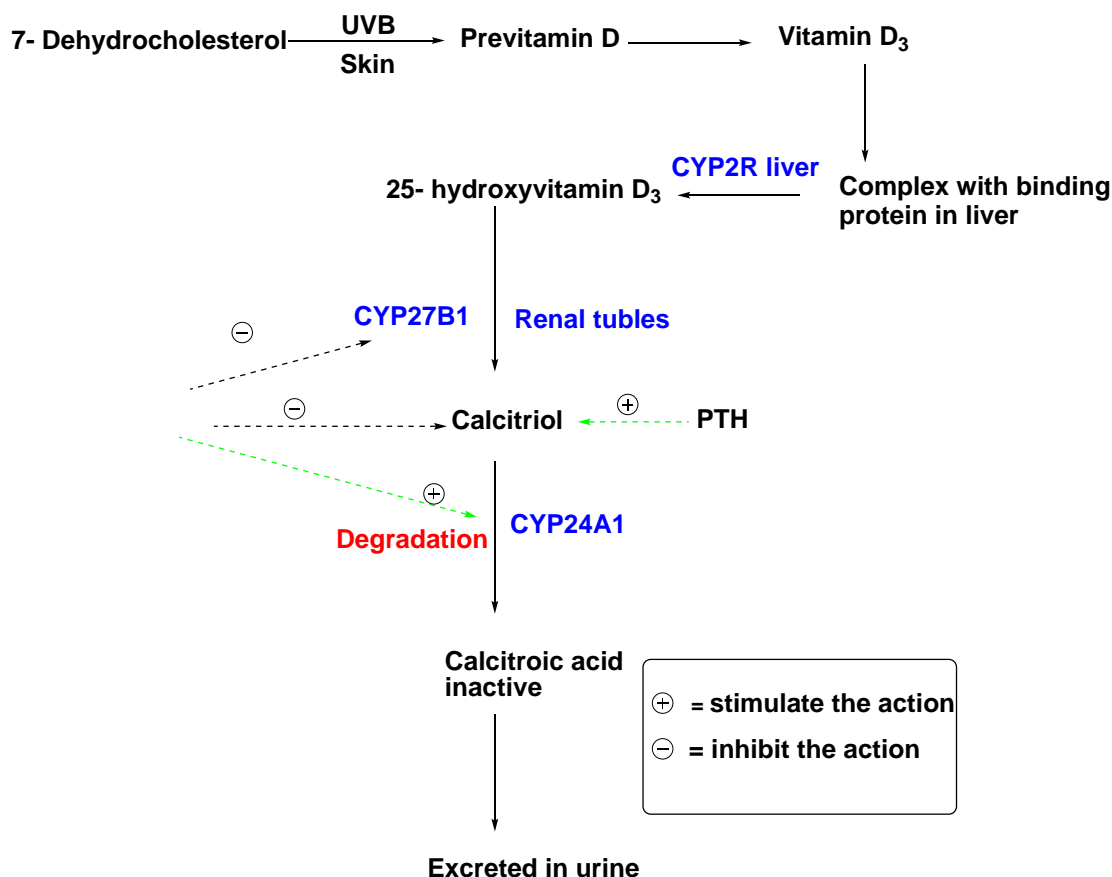


Figure 1. Metabolic pathway of Vitamin D

The initial step in vitamin D metabolism is 25 hydroxylation (endoplasmic reticulum) by CYP2R1 (25-hydroxylase), found in the liver to produce 25(OH)D₃ (the circulatory form of

vitamin D) (Figure 1)². 1,25(OH)₂D₃ (calcitriol), the active form of vitamin D, is produced in the renal distal convoluted tubule at position 1 α by CYP27B1 a cytochrome P450 monooxygenase which helps many reactions involved in drug metabolism and the synthesis of cholesterol, steroids, and other lipids⁵. CYP27B1 is stimulated by parathyroid hormone (PTH) and is indirectly deactivated by fibroblast growth factor (FGF-23) (Figure 1)⁶.

The main function of calcitriol is mineralisation of the skeleton and maintaining levels of calcium^{7,8}. However, calcitriol also plays a role in many other organs with vitamin D deficiency linked to chronic kidney disease^{9,10}, cardiovascular disease^{11,12}, autoimmune disease^{13,14} and cancer^{15,16,17,18,19}. Reduction in calcitriol levels is linked with increased CYP24A1 levels, which suggests that CYP24A1 may be a useful therapeutic target²⁰. Many cancer cell lines display elevated levels of CYP24A1 expression as they progress to more tumourigenic phenotypes, suggesting that these tumours have increased ability to catabolise calcitriol. Subsequently, several CYP24A1 inhibitors have been designed for the treatment of diseases associated with elevated vitamin D catabolism. Azole-based compounds can inactivate a broad range of cytochrome P450 enzymes by binding to the haem moiety present in the enzyme active site. Through the coordination of the azole nitrogen to the haem, it blocks the catalytic cycle of the P450 and prevents oxygen activation required for substrate oxidation. Despite their lack of specificity towards just CYP24A1, ketoconazole and liarazole were shown to extend the half-life of calcitriol in prostate cancer cells *in vitro* and *in vivo*²¹. We have previously described azole CYP24A1 inhibitors^{22,23,24,25}, of these the styrylimidazole series²⁴ was the most promising with potent CYP24A1 inhibitory activity observed (Figure 2). The aim of this research was the design and synthesis of novel potent inhibitors of CYP24A1 to enhance the endogenous levels of circulating calcitriol.

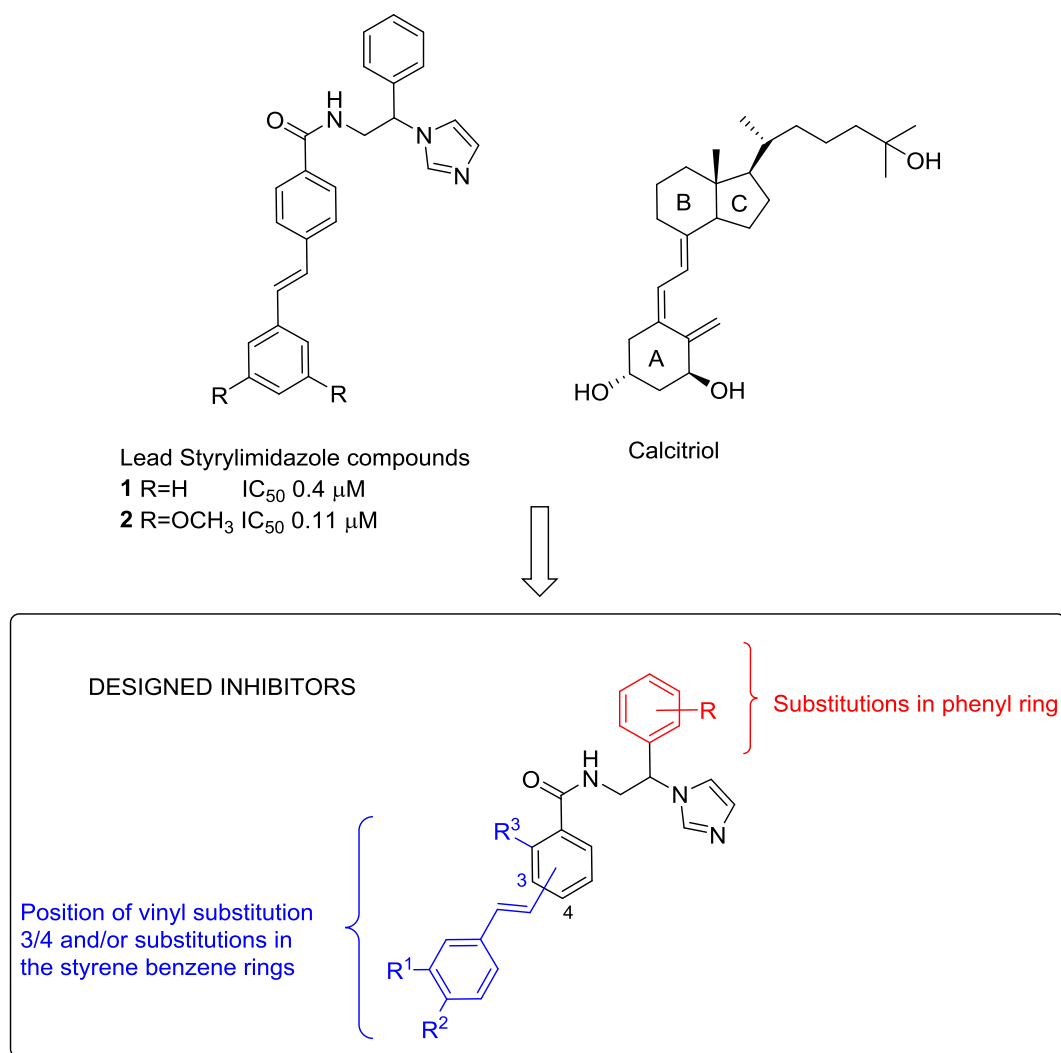


Figure 2. Lead styrylimidazoles and designed inhibitors

The lead styrylimidazoles (Figure 2) have been modified and developed, specifically through (i) substitution of the phenyl ring on the imidazole side to explore structure activity-relationships; (ii) substitution of the styrene benzene rings to explore structure activity-relationships and (iii) variation of the alkene position to allow complete filling of the CYP24A1 active site.

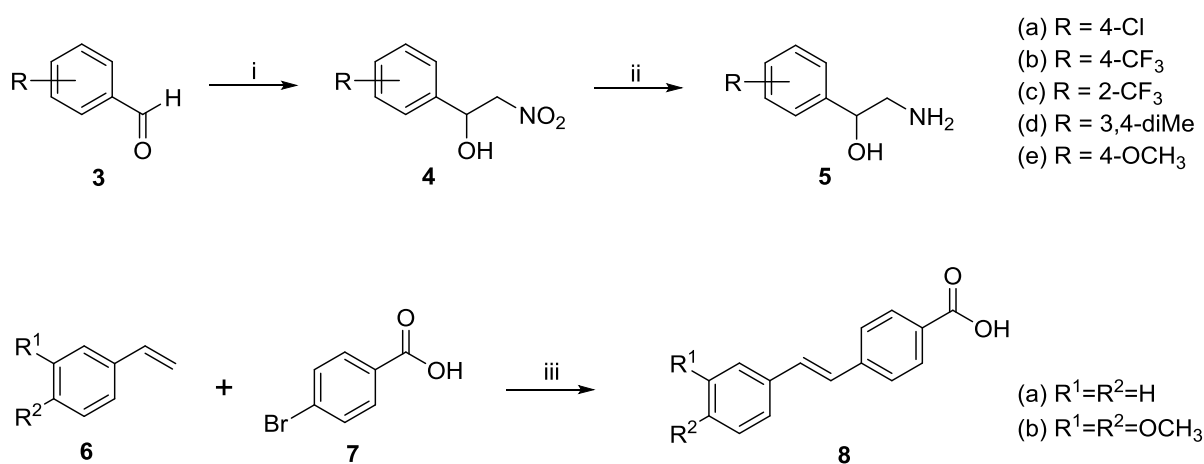
2. Results and Discussion

2.1 Chemistry

Both the 4- and 3-substituted final compounds, (*E*)-*N*-(2-(1*H*-imidazol-1-yl)-2-(phenyl)ethyl)-4-styrylbenzamides (**9**) and (*E*)-*N*-(2-(1*H*-imidazol-1-yl)-2-(phenyl)ethyl)-3-styrylbenzamides (**15**), were obtained in an efficient three step synthesis from the precursor styrylbenzoic acids and 2-amino-1-phenylethanol derivatives.

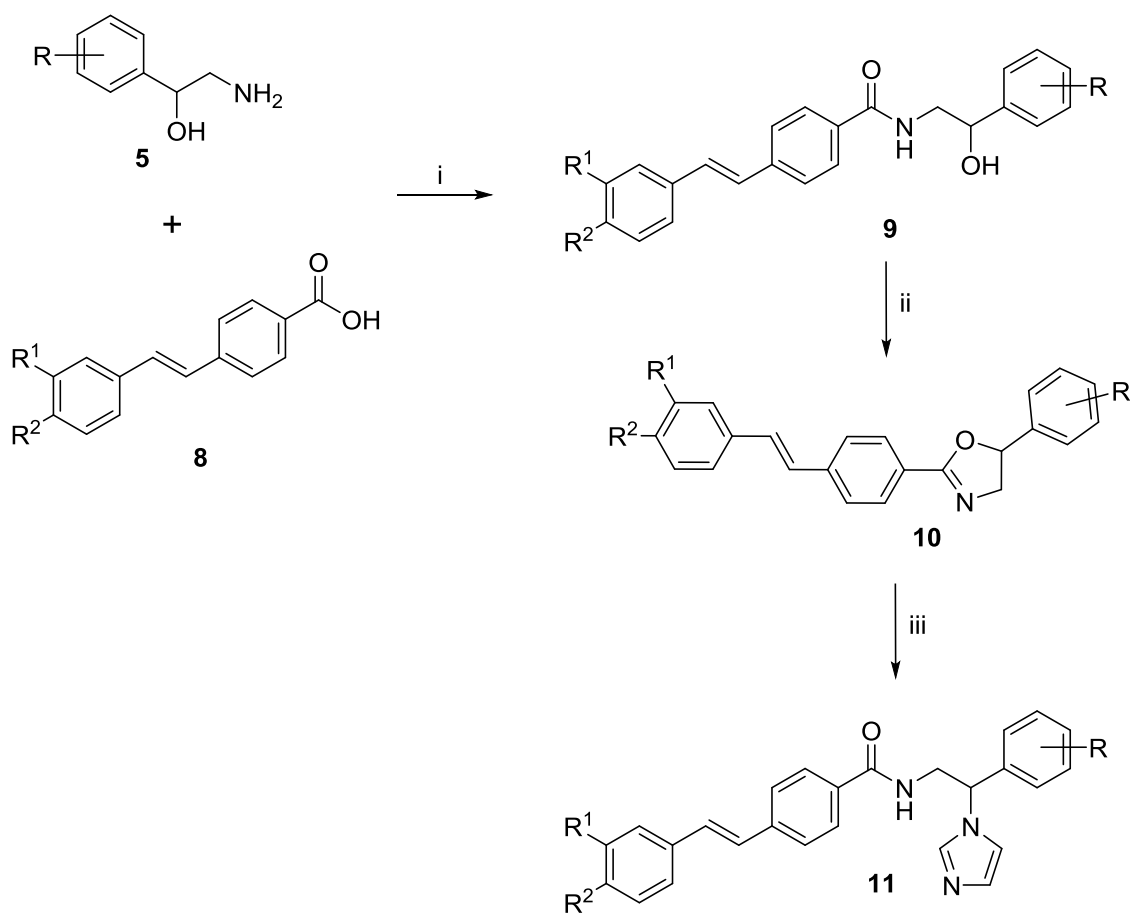
2.1.1. Synthesis of (*E*)-*N*-(2-(1*H*-imidazol-1-yl)-2-(phenyl)ethyl)-4-styrylbenzamides

The extension of the (*E*)-*N*-(2-(1*H*-imidazol-1-yl)-2-(phenyl)ethyl)-4-styrylbenzamide series required coupling of the appropriate 2-amino-1-phenylethanol (**5**) with a 4-styrylbenzoic acid (**8**). The 2-amino-1-phenylethanol derivatives (**5**) were prepared in two steps, first the β -nitroalcohols (**4**) were prepared from the corresponding benzaldehyde (**3**) and nitromethane by the Henry reaction employing either NaOH, Amberseep 900 (OH) or triethylamine as the base^{26,27,28}. Reduction of the β -nitroalcohols to the corresponding amino derivatives (**5**) was achieved using a slurry of Raney nickel and formic acid under H₂ atmosphere at room temperature for 6 h (Scheme 1)²⁹. The 4-styrylbenzoic acids (**8**) were conveniently prepared from the corresponding alkene (**6**) and 4-bromobenzoic acid (**7**) under Heck reaction conditions (Scheme 1).



Scheme 1. Reagents and conditions: (i) Method A CH₃NO₂, MeOH, NaOH, 0 °C, 24 h; Method B CH₃NO₂, Ambersep 900 (OH), rt, o/n; Method C CH₃NO₂, Et₃N, rt, 12 h (ii) Raney Ni/H₂, MeOH, HCO₂H, rt, 6 h (iii) Pd(OAc)₂, tri(o-tolylphosphine), Et₃N, 100 °C, o/n.

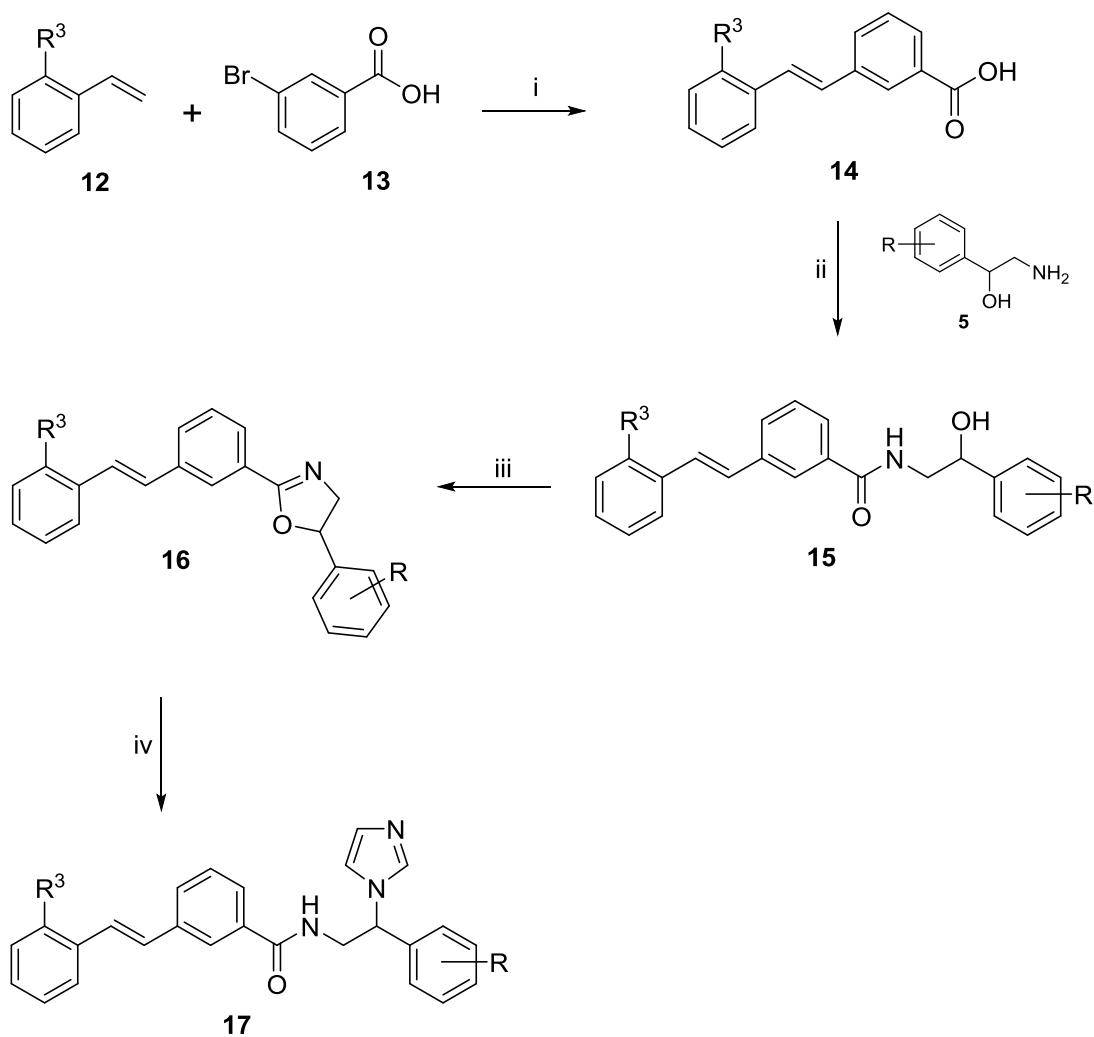
Coupling of the appropriate 2-amino-1-phenylethanol (**5**) with a 4-styrylbenzoic acid (**8**) using CDI as the coupling reagent gave the benzamides (**9**). The dihydrooxazoles (**10**) were prepared following the procedure of Aboraia et al²³ and involved the formation of the 1,3-oxazole ring by reacting benzamide (**9**) with methansulfonyl chloride and triethylamine in dry THF. In the last step of the reaction scheme, heating the oxazole compound (**10**) in the presence of imidazole for 48 h at 125 °C opened the oxazole ring by nucleophilic displacement (Scheme 2)²⁴. A reasonable yield of the imidazole compounds (**11**) was produced after recrystallisation from ethylacetate or acetonitrile (Table 1).



Scheme 2. Reagents and conditions: (i) Carbonyldiimidazole, DMF, rt, o/n (ii) (a) CH₃SO₂Cl, THF, 0 °C, 3 h (b) Et₃N, rt, o/n (iii) imidazole, 125 °C, 48 h.

2.1.2. Synthesis of (*E*)-*N*-(2-(1*H*-imidazol-1-yl)-2-(phenyl)ethyl)-3-styrylbenzamides

In a similar manner the (*E*)-*N*-(2-(1*H*-imidazol-1-yl)-2-(phenyl)ethyl)-3-styrylbenzamide series (**17**) were prepared in moderate yields (Table 1) from the appropriate 3-styrylbenzoic acid (**14**) and 2-amino-1-phenylethanol (**5**) (Scheme 3).



Scheme 3. Reagents and conditions: (i) Pd(OAc)₂, tri(*o*-tolylphosphine), Et₃N, 100 °C, o/n (ii) Carbonyldiimidazole, DMF, rt, o/n (iii) (a) CH₃SO₂Cl, THF, 0 °C, 3 h (b) Et₃N, rt, o/n (iv) imidazole, 125 °C, 48 h.

Table 1. Substitutions, yields and melting points of final imidazole products

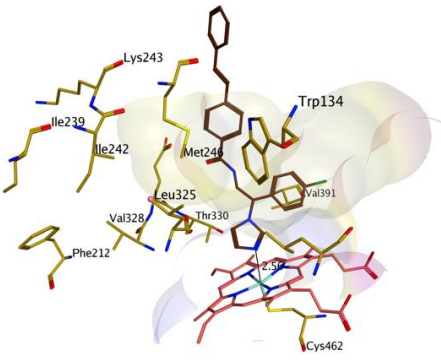
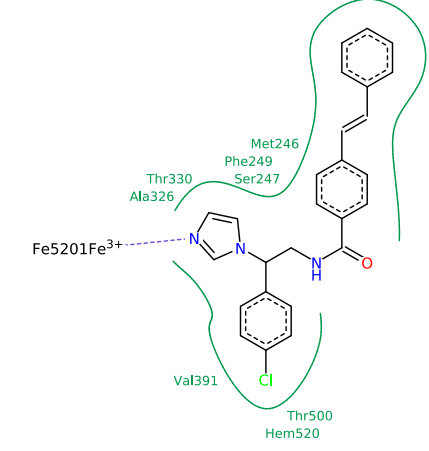
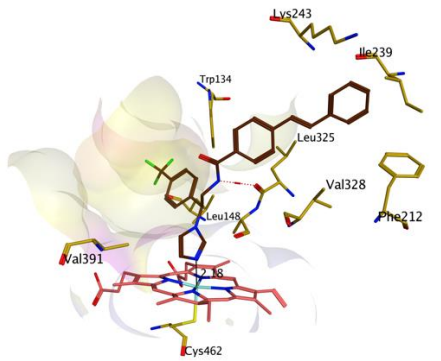
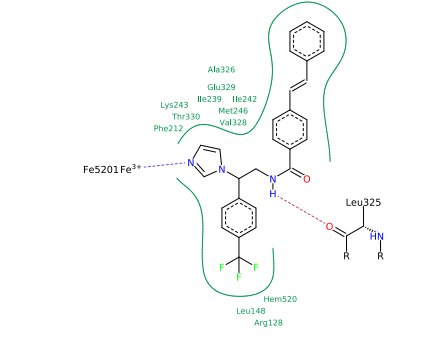
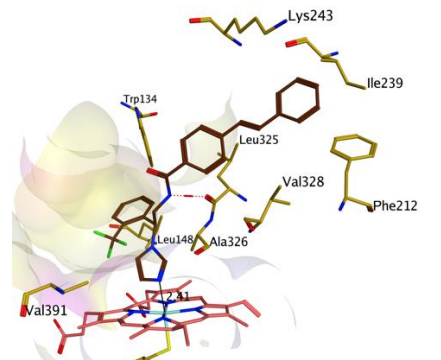
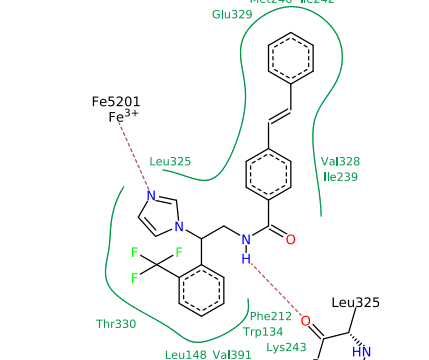
Cmpd	R	R ¹	R ²	R ³	Yield (%)	Mp (°C)
11a	4-Cl	H	H	-	12	238-240
11b	4-CF ₃	H	H	-	33	208-210
11c	2-CF ₃	H	H	-	35	174-178
11d	3,4-diMe	H	H	-	27	134-136
11e	4-OCH ₃	H	H	-	32	218-222
11f	4-Cl	OCH ₃	OCH ₃	-	35	204-208
17a	H	-	-	H	38	158-160
17b	4-Cl	-	-	H	32	148-152
17c	4-CF ₃	-	-	H	48	126-130
17d	H	-	-	CF ₃	33	110-114

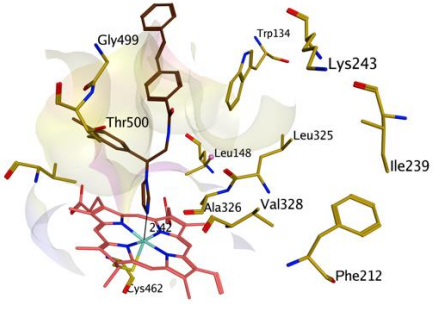
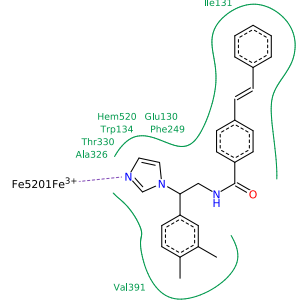
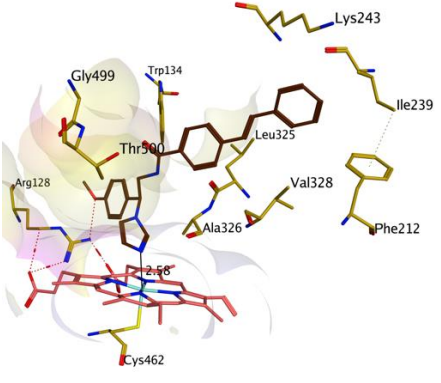
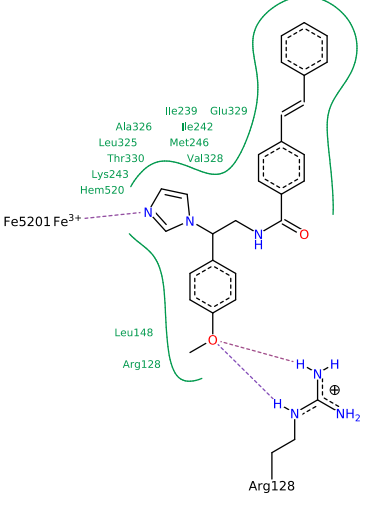
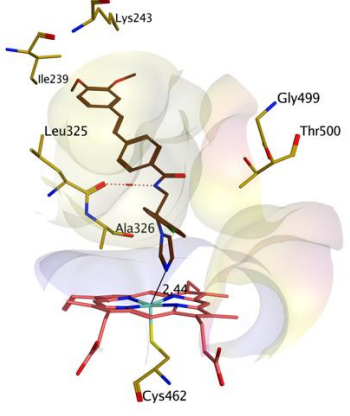
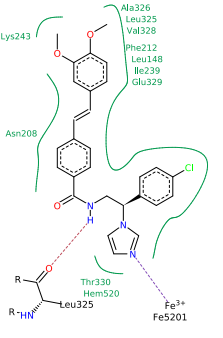
2.2 Molecular modelling

To investigate the possible binding mode of this series of compounds, we have performed a set of molecular docking simulations, using our model of CYP24A1^{24,30}. We have previously shown the importance of the styrylphenyl structure for inhibitory activity and that the imidazole was essential for metal-ligand interaction with the haem group of the enzyme^{23,24,25}. Compounds **11a** - **11f** have electron withdrawing and electron donating substituents on the phenyl ring. All compounds were designed without substitution on styrene group except compound **11f**, which has a 4-Cl on the phenyl ring and 3,4-dimethoxy substitution on the styrene group. All the compounds reached the active site through the vitamin D access tunnel and interacted with multiple hydrophobic residues (Arg128, Glu130, Ile131, Trp134, Leu148, Asn208, Phe212, Ile239, Ile242, Lys243, Met246, Ser247, Phe249, Ala326, Val328, Glu329, The330, Val391 and Thr500). Compounds **11b** - **11d**, formed hydrogen bonds between the

nitrogen of the amide group with Leu325. For compound **11e** an additional hydrogen bond between the methoxy group and Arg128 was observed. The distance between the imidazole ring and the haem iron was between 2.18 Å and 2.58 Å (Table 2).

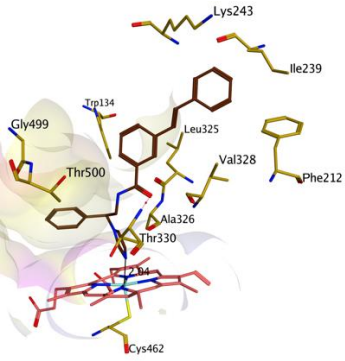
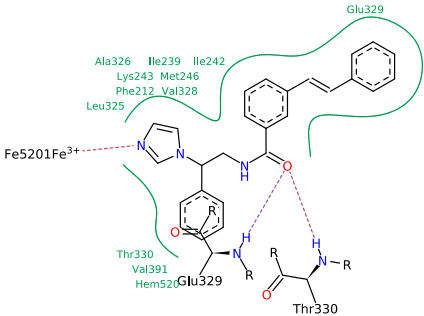
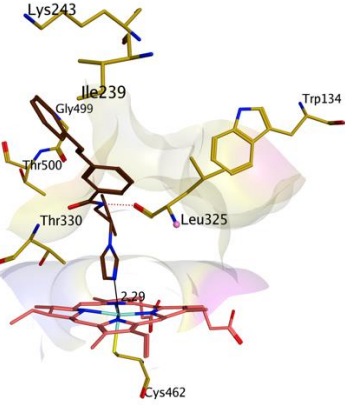
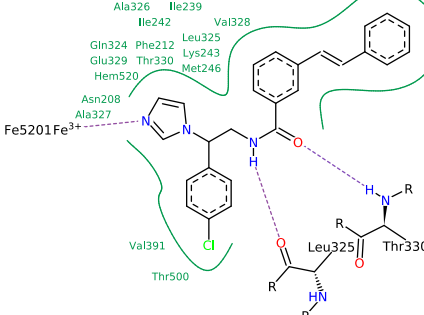
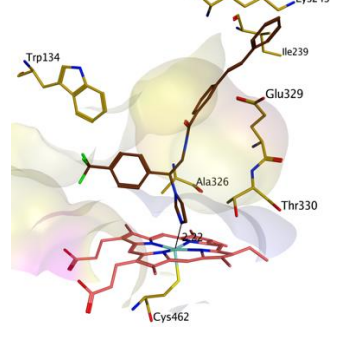
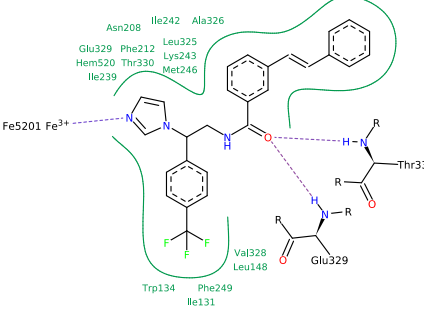
Table 2. (A) Distance between N of heterocycle of compounds **11a-11f** and iron of haem, (B) 3D, (C) 2D with binding interactions and (D) binding energy (kcal/mol)

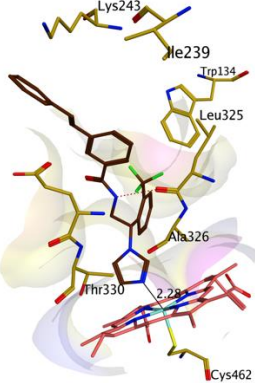
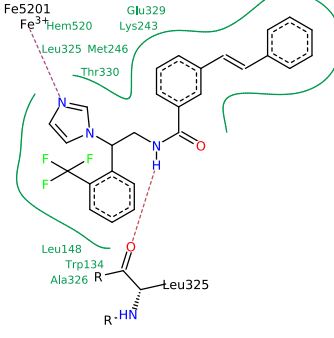
Cpd	A	B	C	D
11a	2.56 Å			-8.9
11b	2.18 Å			-7.1
11c	2.41 Å			-7.9

11d	2.42 Å			-7.4
11e	2.58 Å			-11.2
11f	2.44 Å			-11.8

Compounds **17a** - **17d** were modified by changing the position of the alkene group from the 4 to 3-position. All compound showed good interaction with the active site and interaction between the imidazole nitrogen and the iron of the haem with distances ranging between 2.04 Å and 2.29 Å. Hydrogen bonds were observed between the amide group, through the C=O and/or NH, and amino acids Glu329, Thr330 and Leu325 (Table 3).

Table 3. (A) Distance between N of heterocycle of compounds **17a-17d** and iron of haem, (B) 3D, (C) 2D with binding interactions and (D) binding energy (kcal/mol)

Cpd	A	B	C	D
17a	2.04 Å			-11.0
17b	2.29 Å			-10.4
17c	2.22 Å			-7.3

17d	2.28 Å			-7.6
-----	--------	---	--	------

2.3 CYP24A1 enzyme inhibition

All the final compounds **11a** - **11f** and **17a** - **17d** were evaluated to determine CYP24A1 inhibitory activity. The assay was performed according to the method of Zhu *et al*³¹ and in general, the compounds displayed potent inhibition of CYP24A1 activity when compared with the ketoconazole standard and the lead compound **1** (IC₅₀ 0.40 μM)²⁴. The IC₅₀ values ranged between 11 and 35 μM with the best IC₅₀ value was obtained for the 3,4-dimethoxy styrylbenzamide derivative **11e** (0.11 μM) (Table 4). Interestingly, the 4-methoxy derivative **11e** was also found to interact with the iron of the haem via the methoxy group (distance 2.19 Å), which may contribute to the optimal inhibitory activity in this series of compounds (Figure 3).

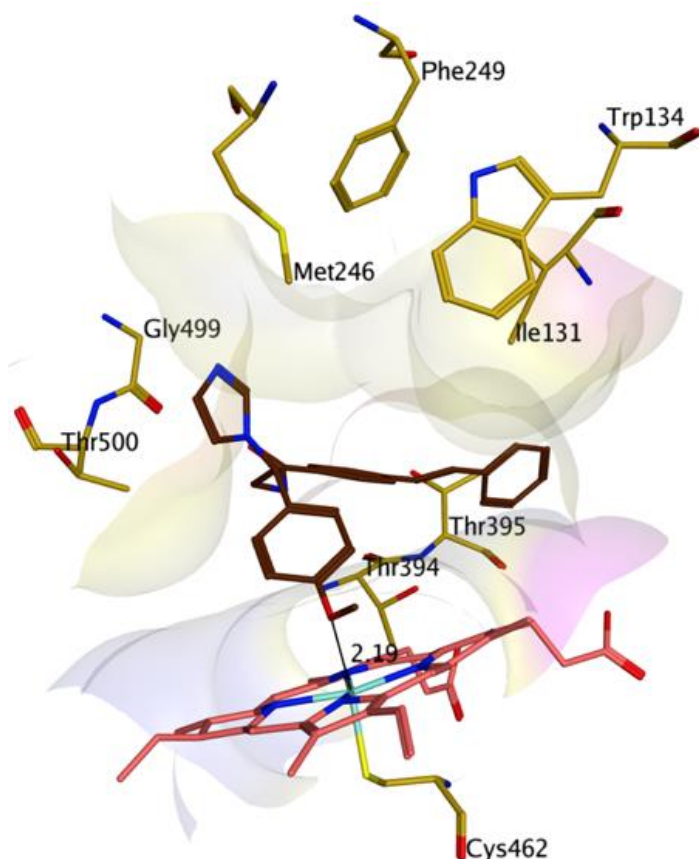
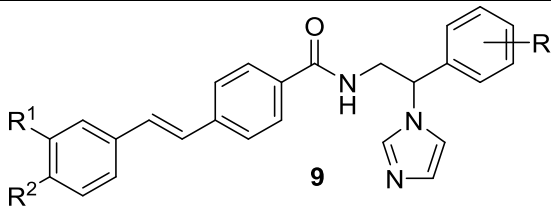
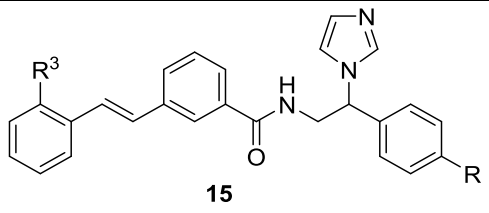


Figure 3. Alternative binding mode of **11e** interacting with the iron of the haem through the methoxy group

The unsubstituted 3-styrylbenzamide showed an improvement in inhibitory activity compared with the 4-styrylbenzamide lead compound **1** (**17a** IC_{50} 0.19 μ M compared with lead **1** IC_{50} 0.40 μ M), whereas the 4-chloro (**17b/11a**) and 4-trifluoromethyl (**17c/11b**) substituted 3- and 4-styrylbenzamides were comparable. In the 4-styrylbenzamide series substitution at the 2-position of the phenyl ring is less favoured e.g. 2- CF_3 **11c** IC_{50} 0.35 μ M compared with 4- CF_3 **11b** IC_{50} 0.18 μ M.

Substitutions in the styryl group would suggest that introduction of substituents at the 3,4-position (**11f** IC_{50} 0.12 μ M) are beneficial for inhibitory activity and comparable with 3,5-dimethoxy substitution (lead **2** IC_{50} 0.11 μ M), while substitutions in the 2-position are less favourable (**17d** IC_{50} 0.34 μ M).

Table 4. IC₅₀ data against CYP24A1 of imidazole derivatives **11** and **17**

								
Cmpd	R	R ¹	R ²	IC ₅₀ (μM)	Cmpd	R	R ³	IC ₅₀ (μM)
11a	4-Cl	H	H	0.21	17a	H	H	0.19
11b	4-CF ₃	H	H	0.18	17b	Cl	H	0.16
11c	2-CF ₃	H	H	0.35	17c	CF ₃	H	0.15
11d	3,4-diMe	H	H	0.31	17d	H	CF ₃	0.34
11e	4-OCH ₃	H	H	0.11	Ketoconazole			0.5
11f	4-Cl	OCH ₃	OCH ₃	0.12				
Lead 1	H	H	H	0.40				

In general, binding energies (Tables 2 and 3) and IC₅₀ showed a good correlation with the exception of compounds **11b** and **17c** (Fig.4). Substitution of these compounds with the more bulky trifluoromethyl group in the para position of the phenyl ring results in a slightly less favourable conformer energy compared with the other inhibitors, which affects the overall binding energy.

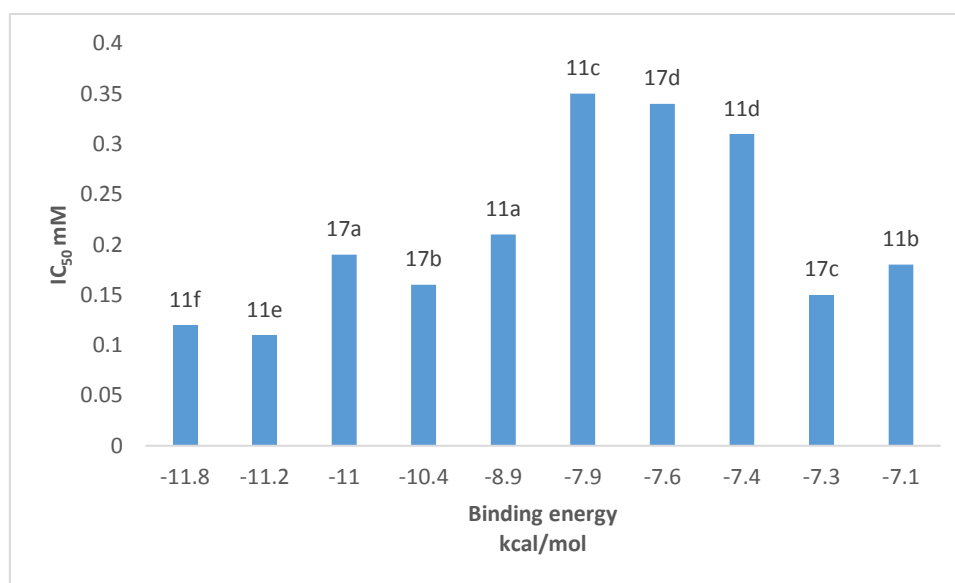


Figure 4. Correlation between CYP24A1 IC₅₀ and binding energy for imidazole derivatives **11** and **17**

3. Conclusions

A series of 3- and 4-styrylbenzamide imidazole derivatives have been prepared using an efficient synthetic route. All the derivatives showed very good inhibitory activity against CYP24A1 and, although there were some small differences in IC_{50} values depending on substituents, overall both 3- and 4-styrylbenzamide imidazoles and a range of substituents were very well tolerated without any significant loss of inhibitory activity. This inhibitory data would agree with the molecular docking where all the compounds fit well within the active site and showed a good fill of the hydrophobic channel of the CYP24A1 active site as well as transition metal interaction between the iron of the haem and the imidazole ring of the derivatives.

4. Experimental

4.1. Chemistry

4.1.1. General Experimental

1,25(OH)₂D₃ and 25(OH)D₃ were purchased from SAFC-Pharma (Madison, WI). Human MBP-CYP24A1, bovine adrenodoxin (Adx), and adrenodoxin reductase (AdR) were purified as described previously³⁰. All solvents used for chromatography were HPLC grade from Fisher Scientific (UK). ¹H and ¹³C NMR spectra were recorded with a Bruker Avance DPX500 spectrometer operating at 500 and 125 MHz, with Me₄Si as internal standard. Mass spectra and microanalysis were determined by MEDAC (Chobham, UK). Flash column chromatography was performed with silica gel 60 (230-400mesh) (Merck) and TLC was carried out on precoated silica plates (kiesel gel 60 F₂₅₄, BDH). Compounds were visualised by illumination under UV light (254 nm) or by the use of vanillin stain followed by charring on a hotplate. Melting points were determined on an electrothermal instrument and are uncorrected. All solvents were dried prior to use and stored over 4Å molecular sieves, under nitrogen. All compounds were more than 95% pure.

4.1.2. General procedure for the preparation of (*E*)-*N*-(2-(4-substitued-phenyl)-2-hydroxyethyl)-4-styrylbenzamides (9) and (*E*)-*N*-(2-hydroxy-2-phenylethyl)-3-styrylbenzamides (15).

A suspension of (*E*)-styrylbenzoic acid (**8** or **14**) (2 mmol) in dry DMF (8 mL) was combined with CDI (2.2 mmol). The reaction was stirred for 1 h at room temperature under nitrogen. The mixture was cooled to 0 °C then added to a solution of 2-amino-1-phenylethan-1-ol (**5**) (2 mmol) in dry DMF (2.5 mL). The resulting mixture was stirred at room temperature overnight and on completion, ice was added into the flask and a white solid precipitated out. The precipitate was then filtered, washed with ice-cold water and dried.

4.1.2.1. (*E*)-*N*-(2-(4-chlorophenyl)-2-hydroxyethyl)-4-styrylbenzamide (9a, R = 4-Cl, R¹ = R² = H). White crystalline solid obtained after recrystallization from methanol. Yield: 67%; R_f 0.86 (CH₂Cl₂-CH₃OH 9:1 v/v); mp 258 - 260 °C; ¹H NMR (DMSO-*d*₆): δ 8.52 (t, *J* = 5.3 Hz, 1H, NH), 7.85 (d, *J* = 8.2 Hz, 2H, Ar), 7.73 (d, *J* = 8.4 Hz, 2H, Ar), 7.74 (d, *J* = 8.2 Hz, 2H, Ar), 7.42 (m, 5H, Ar) 7.24 (m, 4H, Ar), 5.64 (s, 1H, OH), 4.80 (m, 1H, CHOH), 3.49 (m, 1H, CH₂), 3.40 (m, 1H, CH₂). ¹³C NMR (DMSO-*d*₆): δ 167.6 (CO), 140.9, 137.5, 135.2, 133.6, 133.2 (5 × C), 129.4, 128.5, 128.1, 127.3, 127.2, 127.1, 126.9 (15 × CH, Ar), 72.2 (CH), 47.1 (CH₂). Anal. Calcd for C₂₃H₂₀ClNO₂· 0.3H₂O (382.52): C 72.08 %, H 5.42 %, N 3.65 %. Found C 72.20 %, H 5.26 %, N 3.86 %.

4.1.2.2. (*E*)-*N*-(2-hydroxy-2-(4-(trifluoromethyl)phenyl)ethyl)-4-styrylbenzamide (9b, R = 4-CF₃, R¹ = R² = H). White crystalline solid obtained after recrystallization from methanol. Yield: 35%; R_f 0.75 (petroleum ether-EtOAc 3:1 v/v); mp 220 - 224 °C; ¹H NMR (DMSO-*d*₆): δ 8.58 (t, *J* = 5.7 Hz, 1H, NH), 7.84 (d, *J* = 8.4 Hz, 2H, Ar), 7.72 (q, *J* = 8.4, 10.5 Hz, 4H, Ar), 7.65 (m, 4H, Ar), 7.42 (m, 3H, Ar) 7.33 (m, 2H, Ar), 5.77 (d, *J* = 4.5 Hz, 1H, OH), 4.89 (t, *J* = 5.5 Hz, 1H, CHOH), 3.53 (m, 1H, CH₂), 3.43 (m, 1H, CH₂). ¹³C NMR (DMSO-*d*₆): δ 166.6 (CO), 149.0, 140.3, 137.2, 133.6 (4 × C), 129.2, 128.5 (2 × CH, Ar), 128.3, 128.0 (2 × C),

127.9, 127.3, 127.2, 127.1, 126.7, 125.4 (13 × CH, Ar), 71.2 (CH), 47.9 (CH₂). Anal. Calcd for C₂₄H₂₀F₃NO₂ (411.42): C 70.07 %, H 4.90 %, N 3.40 %. Found C 70.39 %, H 4.79 %, N 3.47 %.

4.1.2.3. (*E*)-*N*-(2-hydroxy-2-(2-(trifluoromethyl)phenyl)ethyl)-4-styrylbenzamide (9c, R = 2-CF₃, R¹ = R² = H). White crystalline solid obtained after recrystallization from methanol. Yield: 58%; R_f 0.40 (petroleum ether-EtOAc 3:1 v/v); mp 160 - 166 °C; ¹H NMR (DMSO-d₆): δ 8.58 (t, *J* = 6 Hz, 1H, NH), 7.87 (d, *J* = 8.5 Hz, 3H, Ar), 7.74 (m, 4H, Ar), 7.68 (d, *J* = 15.5 Hz, 2H, Ar), 7.51 (t, *J* = 7.7 Hz, 1H, Ar), 7.42 (m, 2H, Ar), 7.33 (m, 3H, Ar), 5.81 (d, *J* = 4.0 Hz, 1H, OH), 5.14 (dd, *J* = 5.1, 11.9 Hz, 1H, CHOH), 3.51 (m, 2H, CH₂). ¹³C NMR (DMSO-d₆): δ 169.6 (CO), 141 (C), 140.3, 131.0 (CH), 128.8 (C), 128.2, 128.1, 127.8, 127.3, 127.0, 126.3, 126.6, 125.1, 126.7, 125.4 (14 × CH, Ar), 124.3, 123.2 (5 × C), 77.2 (CH), 48.3 (CH₂). Anal. Calcd for C₂₄H₂₀F₃NO₂ (411.42): C 70.07 %, H 4.90 %, N 3.40 %. Found C 70.22 %, H 4.92 %, N 3.38 %.

4.1.2.4. (*E*)-*N*-(2-(3,4-dimethylphenyl)-2-hydroxyethyl)-4-styrylbenzamide (9d, R = 3,4-diCH₃, R¹ = R² = H). White crystalline solid obtained after recrystallization from ethanol. Yield: 60%; R_f 0.80 (CH₂Cl₂-CH₃OH 9.5:0.5 v/v); mp 150 - 154 °C; ¹H NMR (CDCl₃): δ 8.08 (s, 1H, Ar), 8.63 (d, *J* = 8.0 Hz, 1H, Ar), 7.57 (d, *J* = 7.5 Hz, 2H, Ar), 7.42 (t, *J* = 7.5 Hz, 2H, Ar), 7.33 (t, *J* = 7.5 Hz, 2H, Ar), 7.28 (s, 1H, Ar), 7.26 (s, 1H, Ar), 7.19 (d, *J* = 4.5 Hz, 2H, Ar), 7.15 (m, 3H, Ar), 5.88 (t, *J* = 10.0 Hz, 1H, OH), 4.56 (dd, *J* = 10.0, 15.0 Hz, 1H, CHOH), 4.17 (m, 1H, CH₂), 3.93 (dd, *J* = 8.5, 14.5 Hz, 1H, CH₂), 3.5 (s, 6H, 2CH₃). ¹³C NMR (CDCl₃): δ 166.5 (CO), 142.1, 140.1, 137.3, 134.9, 133.7, 131.6 (6 × C), 130.6, 130.3, 129.2, 128.4, 128.2, 128.0, 127.8, 127.2, 126.7 (14 × C, Ar), 68.6 (CH), 47.4 (CH₂), 21.35, 18.71 (2 × CH₃). Anal. Calcd for C₂₅H₂₅NO₂ (371.48): C 80.83 %, H 6.78 %, N 3.77 %. Found C 81.10 %, H 6.78 %, N 3.88 %.

4.1.2.5. (*E*)-*N*-(2-hydroxy-2-(4-methoxyphenyl)ethyl)-4-styrylbenzamide (9e, R = 4-OCH₃, R¹ = R² = H). White crystalline solid obtained after recrystallization from methanol. Yield: 35%; R_f 0.70 (petroleum ether-EtOAc 1:3 v/v); mp 218 - 220 °C; ¹H NMR (DMSO-d₆): δ 8.50 (t, *J* = 5.5 Hz, 1H, NH), 7.87 (d, *J* = 8.3 Hz, 2H, Ar), 7.70 (m, 4H, Ar), 7.65 (m, 3H, Ar), 7.33 (m, 2H, Ar), 7.33 (m, 2H, Ar), 6.92 (d, *J* = 8.3 Hz, 2H), 5.43 (d, *J* = 4.5 Hz, 1H, OH), 4.76 (m, 1H, CHOH), 3.74 (s, 3H, OCH₃), 3.50 (m, 1H, CH₂), 3.34 (m, 1H, CH₂). ¹³C NMR (DMSO-d₆): δ 166.5 (CO), 158.8, 140.2, 137.3, 136.3, 133.8 (5 × C), 130.6, 129.2, 128.5, 128.1, 127.6, 127.2, 114.3 (15 × CH, Ar), 71.2 (CH), 55.4 (OCH₃), 48.2 (CH₂). Anal. Calcd for C₂₄H₂₃NO₃ (373.45): C 77.19 %, H 6.21 %, N 3.75 %. Found C 77.32 %, H 6.02 %, N 3.70 %.

4.1.2.6. (*E*)-*N*-(2-(4-chlorophenyl)-2-hydroxyethyl)-4-(3,4-dimethoxystyryl)benzamide (9f, R = 4-Cl, R¹ = R² = OCH₃). White crystalline solid obtained after recrystallization from acetonitrile. Yield: 69%; R_f 0.20 (petroleum ether-EtOAc 1:1 v/v); mp 168 - 172 °C; ¹H NMR (DMSO-d₆): δ 8.53 (t, *J* = 6.0 Hz, 1H, NH), 7.84 (d, *J* = 8.0 Hz, 2H, Ar), 7.65 (d, *J* = 8.5 Hz, 2H, Ar), 7.40 (s, 2H, Ar), 7.36 (m, 2H, Ar), 7.21 (m, 2H, Ar), 7.00 (m, 3H, Ar), 5.66 (d, *J* = 4.5 Hz, 1H, OH), 4.81 (m, 1H, CHOH), 3.49 (m, 2H, CH₂). ¹³C NMR (DMSO-d₆): δ 166.5 (CO), 149.5, 149.4, 143.3, 133.2, 131.9, 128.2 (6 × C), 130.7 (CH, Ar), 130.2 (C), 128.4, 128.3, 128.2, 126.3, 125.8, 120.7, 112.3, 109.7 (12 × CH, Ar), 71.0 (CH), 47.3 (CH₂). LRMS (ES-TOF) *m/z*: 440 [M^{37Cl} + H]⁺, 438 [M^{35Cl} + H]⁺. HRMS (ES-TOF) Calculated mass: 438.1472 [M + H]⁺, measured mass: 438.1463 [M + H]⁺

4.1.2.7. (*E*)-*N*-(2-hydroxy-2-phenylethyl)-3-styrylbenzamide (15a, R = R³ = H). White crystalline solid obtained after recrystallization from methanol. Yield: 60%; R_f 0.68 (CH₂Cl₂-CH₃OH 9:1 v/v); mp 128 - 132 °C; ¹H NMR (DMSO-d₆): δ 8.64 (t, *J* = 6.0 Hz, 1H, NH), 8.11 (s, 1H, Ar), 7.73 (d, *J* = 8.0 Hz, 2H, Ar), 7.65 (d, *J* = 7.5 Hz, 3H, Ar), 7.49 (t, *J* = 8.0 Hz, 3H,

Ar) 7.42 (t, $J = 7.5$ Hz, 3H, Ar), 7.37 (m, 4H, Ar), 5.64 (s, 1H, OH), 4.80 (m, 1H, CHOH), 3.49 (m, 1H, CH₂), 3.40 (m, 1H, CH₂). ¹³C NMR (DMSO-d₆): δ 166.8 (CO), 144.3, 137.5, 137.3, 135.5 (4 \times C), 129.8, 129.7, 129.3, 129.1, 127.9, 128.5, 128.4, 128.3, 127.5, 127.0, 126.9, 126.5, (16 \times CH, Ar), 71.6 (CH), 48.2 (CH₂). Anal. Calcd for C₂₃H₂₁NO₂ \cdot 0.4 H₂O (350.36): C 78.79 %, H 6.27 %, N 3.99 %. Found C 78.35 %, H 6.56 %, N 3.83 %.

4.1.2.8. (*E*)-*N*-(2-(4-chlorophenyl)-2-hydroxyethyl)-3-styrylbenzamide (15b, R = 4-Cl, R³ = H). Cream crystalline solid obtained after recrystallization from methanol. Yield: 50%; R_f 0.44 (petroleum ether-EtOAc 2:1 v/v); mp 138 - 142 °C; ¹H NMR (DMSO-d₆): δ 8.63 (t, $J = 5.0$ Hz, 1H, NH), 8.09 (s, 1H, Ar), 7.63 (d, $J = 7.5$ Hz, 4H, Ar), 7.48 (t, $J = 8.0$ Hz, 4H, Ar), 7.42 (t, $J = 7.5$ Hz, 3H, Ar) 7.36 (m, 3H, Ar), 5.69 (d, $J = 4.0$ Hz, 1H, OH), 4.83 (m, 1H, CHOH), 3.51 (m, 1H, CH₂), 3.39 (m, 1H, CH₂). ¹³C NMR (DMSO-d₆): δ 166.9 (CO), 138.6, 137.5, 135.8, 134.2, 133.2 (5 \times C), 131.9, 128.7, 128.6, 127.9, 127.3, 127.4, 127.1, 126.9, 126.7, 123.4 (15 \times CH, Ar), 72.2 (CH), 48.9 (CH₂). Anal. Calcd for C₂₄H₂₀ClNO₂ \cdot 0.2 H₂O (381.47): C 72.42 %, H 5.39 %, N 3.67 %. Found C 72.11 %, H 5.36 %, N 3.77 %.

4.1.2.9. (*E*)-*N*-(2-hydroxy-2-(4-(trifluoromethyl)phenyl)ethyl)-3-styrylbenzamide (15c, R = 4-CF₃, R³ = H). White crystalline solid obtained after recrystallization from acetonitrile. Yield: 31%; R_f 0.52 (petroleum ether-EtOAc 2:1 v/v); mp 184 - 186 °C; ¹H NMR (DMSO-d₆): δ 8.66 (t, $J = 5.6$ Hz, 1H, NH), 8.08 (s, 1H, Ar), 7.74 (q, $J = 6.6, 7.7$ Hz, 4H, Ar), 7.64 (q, $J = 8.3, 10.0$ Hz, 4H, Ar), 7.49 (t, $J = 7.7$ Hz, 1H, Ar), 7.42 (t, $J = 7.6$ Hz, 2H, Ar) 7.33 (m, 3H, Ar), 5.80 (d, $J = 4.5$ Hz, 1H, OH), 4.93 (dd, $J = 5.1, 11.9$ Hz, 1H, CHOH), 3.54 (m, 1H, CH₂), 3.44 (m, 1H, CH₂). ¹³C NMR (DMSO-d₆): δ 166.9 (CO), 149.0, 137.5, 137.2, 135.4 (4 \times C), 129.8, 129.7, 129.2, 129.1 (4 \times CH, Ar), 128.3, 128.0 (2 \times C), 127.7, 127.3, 127.2, 127.1, 126.8, 125.9 (11 \times CH, Ar), 71.2 (CH), 47.9 (CH₂). Anal. Calcd for C₂₄H₂₀F₃NO₂ \cdot 0.1H₂O (413.23): C 69.76 %, H 4.93 %, N 3.39 %. Found C 69.51%, H 4.94 %, N 3.42 %.

4.1.2.10. (*E*)-*N*-(2-hydroxy-2-phenylethyl)-3-(2-(trifluoromethyl)styryl)benzamide (15d, $R = H$, $R^3 = CF_3$). White solid obtained after purification by flash column chromatography, product eluted with petroleum ether-EtOAc 1:1 v/v. Yield: 75%; R_f 0.70 (petroleum ether-EtOAc 1:1 v/v); mp 88 - 90 °C; 1H NMR ($CDCl_3$): δ 7.89 (s, 1H, Ar), 7.75 (d, $J = 7.7$ Hz, 1H, Ar), 7.68 (m, 3H, Ar), 7.56 (t, $J = 7.7$ Hz, 2H, Ar), 7.50 (m, 5H, Ar), 7.41 (t, $J = 8$ Hz, 1H, Ar), 7.36 (t, $J = 7.7$ Hz, 1H, Ar) 7.29 (m, 1H, Ar), 4.97 (dd, $J = 3.2, 8.1$ Hz, 1H, \underline{CHOH}), 3.93 (m, 1H, CH_2), 3.55 (m, 1H, CH_2). ^{13}C NMR ($DMSO-d_6$): δ 167.5 (CO), 141.5, 137.3, 136.3 (3 \times C), 133.6, 129.1, 128.7, 128.4, 127.9, 127.6, 125.7 (14 \times CH, Ar), 122.6, 122.2 (2 \times C), 114.3 (CH, Ar), 71.2 (CH), 48.2 (CH_2). Anal. Calcd for $C_{24}H_{20}F_3NO_2$ (411.42): C 70.07%, H 4.90 %, N 3.40 %. Found C 69.99 %, H 5.05 %, N 3.53 %.

4.1.3. General procedure for the preparation of (*E*)-5-(4-substitued-phenyl)-2-(4-styrylphenyl)-4,5-dihydrooxazoles (10) and (*E*)-5-phenyl-2-(3-styrylphenyl)-4,5-dihydrooxazoles (16).

A solution of (*E*)-*N*-(2-hydroxy-2-phenylethyl)-3/4-styrylbenzamide (**9** or **15**) (3.4 mmol) in dry THF (30 mL) was cooled to 0 °C. Then methansulfonylchloride (2.2 mL, 27 mmol) was added and the resulting mixture stirred at 0 °C for 3 h. Triethylamine (6.2 mL, 40.8 mmol) was added dropwise and the solution was stirred overnight at room temperature. The mixture was quenched by the addition of NH_4OH (28 %, 3 mL) and the reaction stirred at room temperature for 30 min. Then THF was removed under reduce pressure and the residue was extracted by EtOAc (100mL) and water (2 \times 100 mL). The organic layer was collected, dried ($MgSO_4$) and concentrated under vacuum. The product was pure enough for use in the next reaction.

4.1.3.1. (*E*)- 5-(4-chlorophenyl)-2-(4-styrylphenyl)-4,5-dihydrooxazole (10a, $R = 4-Cl$, $R^1 = R^2 = H$). Light brown solid obtained. Yield: 40%; R_f 0.47 ($CH_2Cl_2-CH_3OH$ 9:1 v/v); mp 128 - 130 °C; 1H NMR ($DMSO-d_6$): δ 7.94 (d, $J = 8.3$ Hz, 2H, Ar), 7.74 (d, $J = 8.3$ Hz, 2H, Ar), 7.66 (d, $J = 7.4$ Hz, 2H, Ar), 7.48 (d, $J = 8.4$ Hz, 2H, Ar), 7.42 (m, 5H, Ar), 7.32 (dd, $J = 2.6,$

7.3 Hz, 2H, Ar), 5.82 (dd, $J = 3.0, 10.0$ Hz, 1H, CH), 4.48 (dd, $J = 10, 14.9$ Hz, 1H, CH₂), 3.85 (dd, $J = 7.4, 15.0$ Hz, 1H, CH₂).

4.1.3.2. (*E*)- 2-(4-styrylphenyl)-5-(4-(trifluoromethyl)phenyl)-4,5-dihydrooxazole (10b, R = 4-CF₃, R¹ = R² = H). Yellow solid obtained. Yield: 90%; R_f 0.70 (petroleum ether-EtOAc 1:1 v/v); ¹H NMR (DMSO-d₆): δ 7.97 (d, $J = 8.3$ Hz, 2H, Ar), 7.80 (m, 4H, Ar), 7.65 (d, $J = 7.4$ Hz, 4H, Ar), 7.61 (d, $J = 8.3$ Hz, 2H, Ar), 7.34 (m, 3H, Ar), 5.93 (dd, $J = 7.4, 10$ Hz, 1H, CH), 4.53 (dd, $J = 10.0, 15$ Hz, 1H, CH₂), 3.87 (dd, $J = 7.2, 1.00$ Hz, 1H, CH₂).

4.1.3.3. (*E*)- 2-(4-styrylphenyl)-5-(2-(trifluoromethyl)phenyl)-4,5-dihydrooxazole (10c, R = 2-CF₃, R¹ = R² = H). Yellow solid obtained. Yield: 70%; R_f 0.65 (petroleum ether-EtOAc 1:1 v/v); mp 112 - 118 °C; ¹H NMR (DMSO-d₆): δ 8.10 (m, 4H, Ar), 7.89 (m, 3H, Ar), 7.85 (m, 4H, Ar), 7.82 (d, $J = 16.2$ Hz, H, alkene), 7.59 (m, 3H, Ar), 5.71 (dd, $J = 8.0, 10.1$ Hz, 1H, CH), 4.51 (dd, $J = 10.3, 15.0$ Hz, 1H, CH₂), 4.01 (dd, $J = 8.0, 15.0$ Hz, 1H, CH₂).

4.1.3.4. (*E*)-5-(3,4-dimethylphenyl)-2-(4-styrylphenyl)-4,5-dihydrooxazole (10d, R = 3,4-diCH₃, R¹ = R² = H). Light brown solid obtained. Yield: 75%; R_f 0.40 (petroleum ether-EtOAc 1:1 v/v); ¹H NMR (DMSO-d₆): δ 7.97 (d, $J = 8.3$ Hz, 2H, Ar), 7.76 (d, $J = 8.3$ Hz, 2H, Ar), 7.66 (d, $J = 7.4$ Hz, 2H, Ar), 7.42 (t, $J = 7.4$ Hz, 3H, Ar), 7.36 (s, 1H, Ar), 7.33 (t, $J = 7.4$ Hz, 2H, Ar), 7.13 (d, $J = 7.4$ Hz, 2H, Ar), 5.92 (dd, $J = 8.2, 10.1$ Hz, 1H, CH), 4.52 (dd, $J = 10.3, 14.9$ Hz, 1H, CH₂), 3.73 (dd, $J = 8.0, 14.9$ Hz, 1H, CH₂), 2.26 (s, 1H, CH₃), 2.24 (s, 1H, CH₃).

4.1.3.5. (*E*)-5-(4-methoxyphenyl)-2-(4-styrylphenyl)-4,5-dihydrooxazole (10e, R = 4-OCH₃, R¹ = R² = H). Light brown solid obtained. Yield: 90%; R_f 0.55 (petroleum ether-EtOAc 1:1 v/v); mp 144 - 146 °C; ¹H NMR (DMSO-d₆): δ 7.92 (d, $J = 8.3$ Hz, 2H, Ar), 7.73 (d, $J = 8.3$ Hz, 2H, Ar), 7.65 (d, $J = 7.5$ Hz, 2H, Ar), 7.42 (m, 2H, Ar), 7.34 (m, 5H, Ar), 6.98 (d, $J = 8.3$ Hz, 2H, Ar), 5.74 (φt, $J = 7.8, 9.8$ Hz, 1H, CH), 4.26 (m, 1H, CH₂), 4.03 (m, 1H, CH₂), 3.76 (s, 3H, OCH₃).

4.1.3.6. (*E*)-5-(3-chlorophenyl)-2-(3-(3,4-dimethoxystyryl)phenyl)-4,5-dihydrooxazole (10f, R = 4-Cl, R¹ = R² = OCH₃). Light brown solid obtained. Yield: 63%; R_f 0.71 (petroleum ether-EtOAc 1:1 v/v); ¹H NMR (DMSO-d₆): δ 7.59 (d, *J* = 8.4 Hz, 3H, Ar), 7.43 (d, *J* = 7.5 Hz, 2H, Ar), 7.17 (m, 2H, Ar), 7.15 (m, 3H, Ar), 6.73 (m, 3H, Ar), 5.68 (m, 1H, CH), 4.52 (m, 1H, CH₂), 4.1 (m, 1H, CH₂), 3.86 (s, 3H, OCH₃), 3.72 (s, 3H, OCH₃).

4.1.3.7. (*E*)-5-phenyl-2-(3-styrylphenyl)-4,5-dihydrooxazole (16a, R = R³ = H). Cream solid obtained. Yield: 85%; R_f 0.55 (petroleum ether-EtOAc 3:1 v/v); ¹H NMR (DMSO-d₆): δ 8.01 (d, *J* = 7.3 Hz, 2H, Ar), 7.87 (m, 5H, Ar), 7.52 (d, *J* = 7.3 Hz, 2H, Ar), 7.44 (m, 5H, Ar), 7.38 (d, 7.3 Hz, 2H, Ar), 5.66 (dd, *J* = 3.0, 9.7 Hz, 1H, CH), 4.56 (dd, *J* = 9.7, 15.0 Hz, 1H, CH₂), 4.51 (dd, *J* = 7.3, 15.0 Hz, 1H, CH₂).

4.1.3.8. (*E*)-5-(4-chlorophenyl)-2-(3-styrylphenyl)-4,5-dihydrooxazole (16b, R = 4-Cl, R³ = H). Cream solid obtained. Yield: 80%; R_f 0.40 (petroleum ether-EtOAc 1:1 v/v); ¹H NMR (DMSO-d₆): δ 8.19 (d, *J* = 8.5 Hz, 2H, Ar), 7.99 (d, 8.5 Hz, 2H, Ar), 7.50 (m, 2H, Ar), 7.41 (m, 4H, Ar), 7.32 (m, 3H, Ar), 7.18 (m, 3H, Ar), 5.79 (dd, *J* = 8.2, 10.2 Hz, 1H, CH), 4.50 (dd, *J* = 10.2, 15.3 Hz, 1H, CH₂), 4.31 (dd, *J* = 8.2, 15.3 Hz, 1H, CH₂).

4.1.3.9. (*E*)-2-(3-styrylphenyl)-5-(4-(trifluoromethyl)phenyl)-4,5-dihydrooxazole (16c, R = 4-CF₃, R³ = H). Light brown solid obtained. Yield: 92%; R_f 0.57 (petroleum ether-EtOAc 1:1 v/v); ¹H NMR (DMSO-d₆): δ 8.02 (d, *J* = 8.5 Hz, 2H, Ar), 7.56 (d, *J* = 8.5 Hz, 2H, Ar), 7.36 (m, 5H, Ar), 7.17 (m, 3H, Ar), 7.08 (m, 2H, Ar), 7.97 (m, 1H, Ar), 5.51 (dd, *J* = 10.1, 15.0 Hz, 1H, CH), 4.09 (dd, *J* = 8.5, 15.0 Hz, 1H, CH₂), 3.99 (dd, *J* = 8.2, 15.3 Hz, 1H, CH₂).

4.1.3.10. (*E*)-5-phenyl-2-(3-(2-(trifluoromethyl)styryl)phenyl)-4,5-dihydrooxazole (16d, R = H, R³ = CF₃). Light brown solid obtained. Yield: 56%; R_f 0.60 (petroleum ether-EtOAc 1:1 v/v); ¹H NMR (DMSO-d₆): δ 7.95 (d, *J* = 8.3 Hz, 2H, Ar), 7.66 (d, *J* = 8.3 Hz, 2H, Ar), 7.58

(d, $J = 8.3$ Hz, 2H, Ar), 7.52 (d, $J = 8.3$ Hz, 2H, Ar), 7.32 (m, 7H, Ar), 5.80 (dd, $J = 7.7, 10.1$ Hz, 1H, CH), 4.45 (dd, $J = 10.1, 14.9$ Hz, 1H, CH₂), 3.89 (dd, $J = 7.5, 14.9$ Hz, 1H, CH₂).

4.1.4. General procedure for the preparation of (*E*)-*N*-(2-(1*H*-imidazol-1-yl)-2-(phenylethyl)-4-styrylbenzamides (11) and (*E*)-*N*-(2-(1*H*-imidazol-1-yl)-2-(phenylethyl)-3-styrylbenzamides (17).

A mixture of (*E*)-5-(4-chlorophenyl)-2-(3/4-styrylphenyl)-4,5-dihydrooxazole (**10** or **16**) (3 mmol) and imidazole (7.4 g, 110 mmol) was refluxed at 125 °C for 48 h. On completion, the mixture was extracted between EtOAc (100 mL) and brine (2 × 100 mL). The organic layer was dried (MgSO₄) and concentrated under vacuum.

4.1.4.1. (*E*)-*N*-(2-(4-chlorophenyl)-2-(1*H*-imidazol-1-yl)ethyl)-4-styrylbenzamide (11a, **R = 4-Cl, **R**¹ = **R**² = H).** White solid obtained after recrystallization from EtOAc. Yield: 12%; R_f 0.85 (CH₂Cl₂-CH₃OH 9:1 v/v); mp 238 - 240 °C; ¹H NMR (DMSO-*d*₆): δ 8.73 (t, $J = 5.2$ Hz, 1H, NH), 7.86 (s, 1H, imid), 7.77 (d, $J = 8.2$ Hz, 4H, Ar), 7.68 (d, $J = 8.2$ Hz, 3H, Ar), 7.64 (d, $J = 7.5$ Hz, 1H, imid), 7.46 (m, 8H, Ar), 6.92 (s, 1H, imid), 5.70 (dd, $J = 6.5, 8.2$ Hz, 1H, CH), 4.06 (m, 1H, CH₂), 3.44 (m, 1H, CH). ¹³C NMR (DMSO-*d*₆): δ 166.8 (CO), 140.5, 138.7, 133.2, 133.1 (5 × C), 137.2, 130.7, 129.3, 129.2, 129.1, 128.5, 127.9, 127.1, 126.7, 118.7 (18 × CH, Ar), 59.1 (CH), 43.7 (CH₂). LRMS (ES-TOF) *m/z*: 430 [**M**^{37Cl} + H]⁺, 428 [**M**^{35Cl} + H]⁺, 362 [**M**^{-imid} + H]⁺. HRMS (ES-TOF) Calculated mass: 428.1523 [**M** + H]⁺, measured mass: 428.1524 [**M** + H]⁺.

4.1.4.2. (*E*)-*N*-(2-(1*H*-imidazol-1-yl)-2-(4-(trifluoromethyl)phenyl)ethyl)-4-styrylbenzamide (11b, **R = 4-CF₃, **R**¹ = **R**² = H).** Cream solid obtained after recrystallization from EtOAc. Yield: 33%; R_f 0.32 (CH₂Cl₂-CH₃OH 9:1 v/v); mp 208 - 210 °C; ¹H NMR (DMSO-*d*₆): δ 8.80 (t, $J = 5.0$ Hz, 1H, NH), 7.91 (s, 1H, imid), 7.78 (dd, $J = 3.0, 8.5$ Hz, 4H,

Ar), 7.69 (d, $J = 8.5$ Hz, 2H, Ar), 7.64 (d, $J = 7.5$ Hz, 2H, Ar), 7.60 (s, 1H, imid), 7.42 (m, 4H, Ar), 7.32 (m, 3H, Ar), 6.95 (s, 1H, imid), 5.83 (t, $J = 7.5$ Hz, 1H, CH), 4.13 (m, 12 Hz, 2H, CH₂). ¹³C NMR (DMSO-d₆): δ 166.8 (CO), 144.4, 140.5, 137.4, 137.1, 135.4, 133.1 (6 \times C), 130.8, 129.2, 128.5, 128.2, 128.1, 127.9, 127.1, 126.7, 126.1, 118.9 (18 \times CH, Ar), 59.3 (CH), 43.7 (CH₂). Anal. Calcd for C₂₇H₂₂F₃N₃O \cdot 0.15H₂O (463.87): C 69.86 %, H 4.84 %, N 9.05 %. Found C 69.56 %, H 4.79 %, N 8.98 %.

4.1.4.3. (E)-N-(2-(1H-imidazol-1-yl)-2-(2-(trifluoromethyl)phenyl)ethyl)-4-styrylbenzamide (11c, R = 2-CF₃, R¹ = R² = H). Cream solid obtained after recrystallization from EtOAc. Yield: 33%; R_f 0.32 (CH₂Cl₂-CH₃OH 9:1 v/v); mp 208 - 210 °C; ¹H NMR (DMSO-d₆): δ 8.80 (t, $J = 5.0$ Hz, 1H, NH), 7.91 (s, 1H, imid), 7.78 (dd, $J = 3.0, 8.5$ Hz, 4H, Ar), 7.69 (d, $J = 8.5$ Hz, 2H, Ar), 7.64 (d, $J = 7.5$ Hz, 2H, Ar), 7.60 (s, 1H, imid), 7.42 (m, 4H, Ar), 7.32 (m, 3H, Ar), 6.95 (s, 1H, imid), 5.83 (t, $J = 7.5$ Hz, 1H, CH), 4.13 (m, 12 Hz, 2H, CH₂). ¹³C NMR (DMSO-d₆): δ 166.8 (CO), 144.4, 140.5, 137.4, 137.1, 135.4, 133.1 (6 \times C), 130.8, 129.2, 128.5, 128.2, 128.1, 127.9, 127.1, 126.7, 126.1, 118.9 (18 \times CH, Ar), 59.3 (CH), 43.7 (CH₂). Anal. Calcd for C₂₇H₂₂F₃N₃O \cdot 0.15H₂O (463.87): C 69.86 %, H 4.84 %, N 9.05 %. Found C 69.56 %, H 4.79 %, N 8.98 %.

4.1.4.4. (E)-N-(2-(3,4-dimethylphenyl)-2-(1H-imidazol-1-yl)ethyl)-4-styrylbenzamide (11d, R = 3,4-diCH₃, R¹ = R² = H). Yellow solid obtained after recrystallization from EtOAc. Yield: 27%; R_f 0.65 (CH₂Cl₂-CH₃OH 9:1 v/v); mp 134 - 136 °C; ¹H NMR (DMSO-d₆): δ 8.73 (t, $J = 5.5$ Hz, 1H, NH), 7.82 (s, 1H, imid), 7.78 (d, $J = 8.5$ Hz, 2H, Ar), 7.69 (m, 2H, Ar), 7.41 (m, 2H, Ar), 7.33 (m, 5H, Ar), 7.18 (s, 1H, imid), 7.14 (m, 2H, Ar), 7.02 (s, 1H, imid), 6.89 (s, 1H, Ar), 5.59 (dd, $J = 5.5, 9.0$ Hz, 1H, CH), 4.09 (m, 1H, CH₂), 3.94 (m, 1H, CH₂), 2.18 (s, 6H, 2 \times CH₃). ¹³C NMR (DMSO-d₆): δ 167.8 (CO), 157.5, 140.9, 138.7, 137.5, 136.7, 133.4 (6 \times C), 133.2, 130.7, 129.3, 129.2, 129.1, 128.5, 127.9, 127.1, 126.7, 118.7 (17 \times CH, Ar), 59.9

(CH), 43.7 (CH₂), 25.7 (2 × CH₃). LRMS (ES-TOF) *m/z*: 422 [M + H]⁺, 214 [M – C₆H₅–CH=CH–C₆H₄–C=O]⁺. HRMS (ES-TOF) Calculated mass: 422.2251 [M + H]⁺, measured mass: 422.2232 [M + H]⁺.

4.1.4.5. (*E*)-*N*-(2-(1*H*-imidazol-1-yl)-2-(4-methoxyphenyl)ethyl)-4-styrylbenzamide (11e, R = 4-OCH₃, R¹ = R² = H). White solid obtained after recrystallization from EtOAc. Yield: 32%; *R_f* 0.41 (CH₂Cl₂–CH₃OH 9:1 v/v); mp 218 - 222 °C; ¹H NMR (CDCl₃): δ 8.06 (s, 1H, imid), 7.78 (d, *J* = 7.7 Hz, 2H, Ar), 7.52 (d, *J* = 7.5 Hz, 2H, Ar), 7.36 (t, *J* = 7.0 Hz, 2H, Ar), 7.31 (m, 5H, Ar), 7.24 (d, *J* = 8 Hz, 2H, Ar), 7.17 (m, 2H, Ar), 6.94 (d, *J* = 8.0 Hz, 2H, Ar), 5.70 (dd, *J* = 4.0, 9.5 Hz, 1H, CH), 4.34 (m, 1H, CH₂), 4.04 (m, 1H, CH), 3.81 (s, 3H, OCH₃). ¹³C NMR (DMSO–d₆): δ 167.8 (CO), 157.5, 140.9, 138.7, 137.5, 136.7, 133.4 (6 × C), 133.2, 130.7, 129.3, 129.2, 129.1, 128.5, 127.9, 127.1, 126.7, 118.7 (18 × CH, Ar), 59.9 (CH), 55.1 (s, 3H, OCH₃), 43.7 (CH₂). LRMS (ES-TOF) *m/z*: 424 [M + H]⁺, 356 [M-imid]⁺. HRMS (ES-TOF) Calculated mass: 424.2020 [M + H]⁺, measured mass: 424.2016 [M + H]⁺.

4.1.4.6. (*E*)-*N*-(2-(4-chlorophenyl)-2-(1*H*-imidazol-1-yl)ethyl)-4-(3,4-dimethoxystyryl)benzamide (11e, R = 4-Cl, R¹ = R² = OCH₃). White solid obtained after recrystallization from acetonitrile. Yield: 35%; *R_f* 0.66 (CH₂Cl₂–CH₃OH 9:1 v/v); mp 204 - 208 °C; ¹H NMR (DMSO–d₆): δ 8.74 (t, *J* = 5.4 Hz, 1H, NH), 7.86 (s, 1H, imid), 7.75 (d, *J* = 8.4 Hz, 2H, Ar), 7.64 (d, *J* = 8.4 Hz, 2H, Ar), 7.46 (m, 2H, Ar), 7.37 (s, 1H, imid), 7.32 (s, 2H, Ar), 7.29 (d, *J* = 5.1 Hz, 2H, Ar), 7.17 (s, 1H, imid), 7.14 (dd, *J* = 1.8, 8.4 Hz, 1H, Ar), 6.98 (d, *J* = 8.4 Hz, 2H, Ar), 6.92 (s, 1H, Ar), 5.71 (dd, *J* = 6.3, 8.7 Hz, 1H, CH), 4.08 (m, 2H, CH₂), 3.83 (s, 3H, OCH₃), 3.78 (s, 3H, OCH₃). ¹³C NMR (DMSO–d₆): δ 166.8 (CO), 149.5, 149.4, 140.9, 138.8 (4 × C), 137.3 (CH, Ar), 133.2, 132.6 (2 × C), 130.8 (CH, Ar), 130.1 (C), 129.3, 129.2, 129.1, 128.1, 126.3, 120.8, 118.7, 112.1, 109.6 (14 × CH, Ar), 59.2 (CH), 43.7 (CH₂). LRMS (ES-TOF) *m/z*: 490 [M³⁷Cl + H]⁺, 488 [M³⁵Cl + H]⁺. HRMS (ES-TOF) Calculated mass: 488.1743 [M + H]⁺, measured mass: 488.1741 [M + H]⁺.

4.1.4.7. (*E*)-*N*-(2-(1*H*-imidazol-1-yl)-2-phenylethyl)-3-styrylbenzamide (17a, R = R³ = H).

White solid obtained after recrystallization from EtOAc. Yield: 38%; R_f 0.27 (CH₂Cl₂-CH₃OH 9:1 v/v); mp 158 - 160 °C; ¹H NMR (DMSO-*d*₆): δ 8.82 (t, *J* = 5.7 Hz, 1H, NH), 7.97 (s, 1H, Ar), 7.75 (d, *J* = 8.0 Hz, 1H, Ar), 7.64 (d, *J* = 8.0 Hz, 4H, Ar), 7.47 (s, 1H, Ar), 7.42 (m, 7H, Ar), 7.35 (m, 4H, Ar), 6.92 (s, 1H, imid), 5.71 (dd, *J* = 6.0, 9.5 Hz, 1H, CH), 4.13 (m, 1H, CH₂), 4.02 (m, 1H, CH₂). ¹³C NMR (DMSO-*d*₆): δ 167.2 (CO), 139.7, 137.6 (2 × C), 137.3 (CH, Ar), 137.2, 135.2 (2 × C), 129.9, 129.8, 129.6, 129.2, 128.5, 128.3, 128.1, 127.7, 127.4, 126.7, 126.3, 125.5, 118.9 (18 × CH, Ar), 59.9 (CH), 43.9 (CH₂). Anal. Calcd for C₂₆H₂₃N₃O · 0.25 H₂O (397.99): C 78.47 %, H 5.95 %, N 10.56 %. Found C 78.17 %, H 5.95 %, N 10.56.

4.1.4.8. (*E*)-*N*-(2-(4-chlorophenyl)-2-(1*H*-imidazol-1-yl)ethyl)-3-styrylbenzamide (17b, R = 4-Cl, R³ = H).

White solid obtained after recrystallization from EtOAc. Yield: 32%; R_f 0.8 (CH₂Cl₂-CH₃OH 9:1 v/v); mp 148 - 152 °C; ¹H NMR (DMSO-*d*₆): δ 8.82 (t, *J* = 5.5 Hz, 1H, NH), 7.95 (s, 1H, imid), 7.88 (s, 1H, Ar), 7.75 (d, *J* = 7.5 Hz, 2H, Ar), 7.47 (m, 5H, Ar), 7.31 (m, 8H, Ar), 6.93 (s, 1H, imid), 5.71 (dd, *J* = 6.0, 8.5 Hz, 1H, CH), 4.11 (m, 1H, CH), 3.91 (m, 1H, CH₂). ¹³C NMR (DMSO-*d*₆): δ 167.2 (CO), 138.7, 137.6 (2 × C), 137.2 (CH, Ar), 137.1, 135.1, 133.2 (3 × C), 129.9, 129.8, 129.4, 192.2, 129.1, 129.0, 128.4, 128.4, 128.1, 127.1, 126.7, 125.5, 118.8 (17 × CH, Ar), 59.1 (CH), 43.7 (CH₂). Anal. Calcd for C₂₆H₂₂ClN₃O (427.93): C 72.98 %, H 5.18 %, N 9.81 %. Found C 72.77 %, H 5.36 %, N 9.40.

4.1.4.9. (*E*)-*N*-(2-(1*H*-imidazol-1-yl)-2-(4-(trifluoromethyl)phenyl)ethyl)-3-styrylbenzamide (17c, R = 4-CF₃, R³ = H).

White solid obtained after recrystallization from EtOAc. Yield: 48%; R_f 0.6 (CH₂Cl₂-CH₃OH 9:1 v/v); mp 126 - 130 °C; ¹H NMR (DMSO-*d*₆): δ 8.84 (t, *J* = 5.5 Hz, 1H, NH), 7.96 (m, 2H, Ar), 7.78 (m, 4H, Ar), 7.64 (m, 5H, Ar), 7.49 (m, 4H, Ar), 7.33 (m, 2H, Ar), 6.96 (s, 1H, imid), 5.84 (m, 1H, CH), 4.15 (m, 2H, CH₂). ¹³C NMR (DMSO-*d*₆): δ 166.9 (CO), 149.0, 144.4, 137.6, 137.5, 135.4, 135.1, 134.9 (7 × C),

129.9, 129.8, 129.7, 129.2, 129.1, 128.4, 128.3, 128.2, 128.1, 127.3, 127.0, 126.1, 125.5, 125.4, 118.9 (18 × CH, Ar), 59.3 (CH), 43.7 (CH₂). LRMS (ES-TOF) m/z: 462 [M + H]⁺, 120 [C₆H₅CONH⁺ + H]⁺. HRMS (ES-TOF) Calculated mass: 462.1793 [M + H]⁺, measured mass: 462.1799 [M + H]⁺.

4.1.4.10. (E)-N-(2-(1H-imidazol-1-yl)-2-phenylethyl)-3-(2-(trifluoromethyl)styryl) benzamide (17d, R =H, R³ = CF₃). White solid obtained after recrystallization from EtOAc. Yield: 33%; R_f 0.5 (CH₂Cl₂-CH₃OH 9:1 v/v); mp 110 - 114 °C; ¹H NMR (DMSO-d₆): δ 8.87 (t, J = 5.5 Hz, 1H, NH), 8.02 (d, J = 7.5 Hz, 2H, Ar), 7.86 (s, 1H, IMID), 7.78 (m, 4H, Ar), 7.54 (m, 5H, Ar), 7.40 (m, 5H, Ar), 6.91 (s, 1H, Ar) 5.71 (dd, J = 6.0, 9.0 Hz, 1H, CH), 4.12 (m, 2H, CH₂). ¹³C NMR (DMSO-d₆): δ 167.9 (CO), 149.0, 144.4, 138.6, 138.5, 136.4, 134.9 (6 × C), 129.9, 129.8, 129.7, 129.2, 129.1, 128.4, 128.3, 128.2, 128.1, 127.3, 127.0, 126.1, 125.5, 125.4, 12.4 (18 × CH, Ar), 59.3 (CH), 43.7 (CH₂). LRMS (ES-TOF) m/z: 462 [M + H]⁺, 394 [M-imidazole]⁺. HRMS (ES-TOF) Calculated mass: 462.1793 [M + H]⁺, measured mass: 462.1795 [M + H]⁺.

4.2. CYP24A1 inhibition assay

Inhibition of CYP24A1 was performed as previously described³¹. Briefly, reaction mixture containing 0.1 μM each of Adx and AdR, 0.075 μM MBP-CYP24A1, 2.5 μM 1,25(OH)₂D₃, varying concentrations of inhibitors, and 0.5 mM NADPH was incubated at 37 °C for 25 min in a buffer of 20 mM Tris (pH 7.5) and 125 mM NaCl. All inhibitors were dissolved in ethanol (>10 mM) or DMSO (>50 mM) and further diluted in ethanol to make working stock (<1 mM). The reaction was extracted with CH₂Cl₂ and analysed by HPLC. The IC₅₀ values were determined by fitting the relative activity (V/V₀) against the inhibitor concentration [I] using the equation $V/V_0 = IC_{50}/(IC_{50} + [I])$, where V and V₀ are the reaction

rates in the presence and absence of inhibitors. The assay for each compound was performed in at least duplicate and in triplicate for compounds with good inhibitory properties.

4.3. Molecular modelling

Docking studies were performed using LeadIT2.1.2 docking program by BioSolve.IT³². The important amino acid residues of the active pocket (Gln82, Ile131, Trp134, Met246, Ala326, Glu329, Thr330, Val391, Phe393, Thr394, Ser498, Gly499, Tyr500)³⁰ were selected and then the selection was extended to 12 Å in order to include in the docking site the haem iron region and the access tunnel to the catalytic site. A ligands database in mol2 format, prepared using MOE³³, was used as input for the docking calculations. The iron atom of the catalytic site was set as essential pharmacophoric feature. Ligand docking was performed using the default values and no water molecules were considered. Ten output solutions were obtained from each compound and visual inspection in MOE was used to identify the interaction between ligand and protein.

Acknowledgements

We acknowledge the Cultural Attaché, Libyan Embassy, London and Misurata University for a PhD scholarship to Ismail M. Taban.

Supplementary material

Supplementary data associated with this article can be found, in the online version, at

.....

References

- (1) Moy, F.-M.; Bulgiba, A. High Prevalence of Vitamin D Insufficiency and Its Association with Obesity and Metabolic Syndrome among Malay Adults in Kuala Lumpur, Malaysia. *BMC Public Health* **2011**, *11* (1), 735.
- (2) Christakos, S.; Ajibade, D. V.; Dhawan, P.; Fechner, A. J.; Mady, L. J. Vitamin D: Metabolism. *Endocrinol. Metab. Clin. North Am.* **2010**, *39* (2), 243–253.
- (3) Bikle, D. D. Vitamin D Metabolism, Mechanism of Action, and Clinical Applications. *Chem. Biol.* **2014**, *21* (3), 319–329.
- (4) Kulie, T.; Groff, A.; Redmer, J.; Hounshell, J.; Schrager, S. Vitamin D: An Evidence-Based Review. *J. Am. Board Fam. Med.* **2009**, *22* (6), 698–706.
- (5) Brożyna, A. A.; Jóźwicki, W.; Janjetovic, Z.; Slominski, A. T. Expression of Vitamin D-Activating Enzyme 1 α -Hydroxylase (CYP27B1) Decreases during Melanoma Progression. *Hum. Pathol.* **2013**, *44* (3), 374–387.
- (6) Powe, C. E.; Ricciardi, C.; Berg, A. H.; Erdenesanaa, D.; Collerone, G.; Ankers, E.; Wenger, J.; Karumanchi, S. A.; Thadhani, R.; Bhan, I. Vitamin D–Binding Protein Modifies the Vitamin D–Bone Mineral Density Relationship. *J. Bone Miner. Res.* **2011**, *26* (7), 1609–1616.
- (7) Melamed, M. L.; Kumar, J. Low Levels of 25-Hydroxyvitamin D in the Pediatric Populations: Prevalence and Clinical Outcomes. *Ped. Health* **2010**, *4* (1), 89–97.
- (8) Driver, J. P.; Foreman, O.; Mathieu, C.; Van Etten, E.; Serreze, D. V. Comparative Therapeutic Effects of Orally Administered 1,25-Dihydroxyvitamin D₃ and 1 α -Hydroxyvitamin D₃ on Type-1 Diabetes in Non-Obese Diabetic Mice Fed a Normal-Calcaemic Diet. *Clin. Exp. Immunol.* **2008**, *151* (1), 76–85.
- (9) Mackawy, A. M. H.; Badawi, M. E. H. Association of Vitamin D and Vitamin D Receptor Gene Polymorphisms with Chronic Inflammation, Insulin Resistance and

- Metabolic Syndrome Components in Type 2 Diabetic Egyptian Patients. *Meta Gene* **2014**, 2, 540–556.
- (10) Bailey, R.; Cooper, J. D.; Zeitels, L.; Smyth, D. J.; Yang, J. H. M.; Walker, N. M.; Hyppönen, E.; Dunger, D. B.; Ramos-Lopez, E.; Badenhoop, K.; Nejentsev, S.; Todd, J. A. Association of the Vitamin D Metabolism Gene CYP27B1 with Type 1 Diabetes. *Diabetes* **2007**, 56 (10), 2616–2621.
 - (11) Fetahu, I. S.; Höbaus, J.; Kállay, E. Vitamin D and the Epigenome. *Front. Physiol.* **2014**, 5 (164), 1–12.
 - (12) Adams, J. M.; Cory, S. The Bcl-2 Apoptotic Switch in Cancer Development and Therapy. *Oncogene* **2007**, 26 (9), 1324–1337.
 - (13) Wijngaarden, T. V.; Pols, H. A. P.; Buurman, C. J.; van den Bemd, G. J. C. M.; Dorssers, L. C. J.; Birkenhäger, J. C.; van Leeuwen, J. P. T. M. Inhibition of Breast Cancer Cell Growth by Combined Treatment with Vitamin D Analogues and Tamoxifen. *Cancer Res.* **1994**, 54 (21), 5711 LP-5717.
 - (14) Benbrahim-Tallaa, L.; Waalkes, M. P. Inorganic Arsenic and Human Prostate Cancer. *Environ. Health Perspect.* **2008**, 116 (2), 158–164.
 - (15) Hamamoto, H.; Kusudo, T.; Urushino, N.; Masuno, H.; Yamamoto, K.; Yamada, S.; Kamakura, M.; Ohta, M.; Inouye, K.; Sakaki, T. Structure-Function Analysis of Vitamin D 24-Hydroxylase (CYP24A1) by Site-Directed Mutagenesis: Amino Acid Residues Responsible for Species-Based Difference of CYP24A1 between Humans and Rats. *Mol. Pharmacol.* **2006**, 70 (1), 120 LP-128.
 - (16) Grahn, R. A.; Ellis, M. R.; Grahn, J. C.; Lyons, L. A. A Novel CYP27B1 Mutation Causes a Feline Vitamin D-Dependent Rickets Type IA. *J. Feline Med. Surg.* **2012**, 14 (8), 587–590.
 - (17) Masudata, S.; Strugnelli, S.; Calverley, M. J.; Makin, H. L. J.; Kremer, R.; Jones, G. In

- Vitro Metabolism of the Anti-Psoriatic Vitamin D Analog, Calcipotriol, in Two Cultured Human Keratinocyte Models. *J. Biol. Chem.* **1994**, 269 (7), 4794–4803.
- (18) Tominaga, Y. Current Status of Parathyroidectomy for Secondary Hyperparathyroidism in Japan. *NDT Plus* **2008**, 1 (Suppl 3), iii35-iii38.
- (19) Murayama, E.; Miyamoto, K.; Kubodera, N.; Mori, T.; Matsunaga, I. Synthetic Studies of Vitamin D3 Analogues. VIII. : Synthesis of 22-Oxavitamin D3 Analogues. *Chem. Pharm. Bull. (Tokyo)*. **1986**, 34 (10), 4410–4413.
- (20) Bosworth, C.; de Boer, I. H. Impaired Vitamin D Metabolism in CKD. *Semin. Nephrol.* **2013**, 33 (2), 158–168.
- (21) Ben-Eltriki, M.; Deb, S.; Guns, E. S. T. Calcitriol in Combination Therapy for Prostate Cancer: Pharmacokinetic and Pharmacodynamic Interactions. *J. Cancer* **2016**, 7 (4), 391–407.
- (22) Yee, S. W.; Simons, C. Synthesis and CYP24 Inhibitory Activity of 2-Substituted-3,4-Dihydro-2*H*-Naphthalen-1-One (Tetralone) Derivatives. *Bioorg. Med. Chem. Lett.* **2004**, 14 (22), 5651–5654.
- (23) Aboraia, A. S.; Yee, S. W.; Gomaa, M. S.; Shah, N.; Robotham, A. C.; Makowski, B.; Prosser, D.; Brancale, A.; Jones, G.; Simons, C. Synthesis and CYP24A1 Inhibitory Activity of N-(2-(1*H*-Imidazol-1-yl)-2-Phenylethyl)arylamides. *Bioorg. Med. Chem.* **2010**, 18 (14), 4939–4946.
- (24) Ferla, S.; Aboraia, A. S.; Brancale, A.; Pepper, C. J.; Zhu, J.; Ochalek, J. T.; DeLuca, H. F.; Simons, C. Small-Molecule Inhibitors of 25-Hydroxyvitamin D-24-Hydroxylase (CYP24A1): Synthesis and Biological Evaluation. *J. Med. Chem.* **2014**, 57 (18), 7702–7715.
- (25) Ferla, S.; Gomaa, M. S.; Brancale, A.; Zhu, J.; Ochalek, J. T.; DeLuca, H. F.; Simons, C. Novel Styryl-Indoles as Small Molecule Inhibitors of 25-Hydroxyvitamin D-24-

- Hydroxylase (CYP24A1): Synthesis and Biological Evaluation. *Eur. J. Med. Chem.* **2014**, 87, 39–51.
- (26) Langer, O.; Dollé, F.; Valette, H.; Halldin, C.; Vaufrey, F.; Fuseau, C.; Coulon, C.; Ottaviani, M.; Någren, K.; Bottlaender, M.; Mazière, B.; Crouzel, C. Synthesis of High-Specific-Radioactivity 4- and 6-[18F]fluorometaraminol- PET Tracers for the Adrenergic Nervous System of the Heart. *Bioorg. Med. Chem.* **2001**, 9 (3), 677–694.
- (27) Lodh, R.; Sarma, M. J.; Borah, A. J.; Phukan, P. Selective Synthesis of Nitroalcohols in the Presence of Ambersep 900 OH as Heterogeneous Catalyst. *Monatshefte für Chemie - Chem. Mon.* **2015**, 146 (6), 969–972.
- (28) Bhabak, K. P.; Arenz, C. Novel Amide- and Sulfonamide-Based Aromatic Ethanolamines: Effects of Various Substituents on the Inhibition of Acid and Neutral Ceramidases. *Bioorg. Med. Chem.* **2012**, 20 (20), 6162–6170.
- (29) Gowda, D. C.; Prakasha Gowda, A. S.; Baba, A. R.; Gowda, S. Nickel-Catalyzed Formic Acid Reductions. A Selective Method for the Reduction of Nitro Compounds. *Synth. Commun.* **2000**, 30 (16), 2889–2895.
- (30) Gomaa, M. S.; Brancale, A.; Simons, C. Homology Model of 1 α ,25-Dihydroxyvitamin D₃ 24-Hydroxylase Cytochrome P450 24A1 (CYP24A1): Active Site Architecture and Ligand Binding. *J. Steroid Biochem. Mol. Biol.* **2007**, 104 (1–2), 53–60.
- (31) Zhu, J.; Barycki, R.; Chiellini, G.; DeLuca, H. F. Screening of Selective Inhibitors of 1 α ,25-Dihydroxyvitamin D₃ 24-Hydroxylase Using Recombinant Human Enzyme Expressed in Escherichia Coli. *Biochemistry* **2010**, 49 (49), 10403–10411.
- (32) <http://www.biosolveit.de/>.
- (33) http://www.chemcomp.com/MOE-Molecular_Operating_Environment.htm.